Pure appl. geophys. 163 (2006) 1495–1513
0033–4553/06/081495–19
DOI 10.1007/s00024-006-0089-z

Pure and Applied Geophysics

Seismic Moment Tensor Resolution on a Local Scale: Simulated Rockburst and Mine-induced Seismic Events in the Kopanang Gold Mine, South Africa

Jan Šílený[1] and Alexander Milev[2]

Abstract—Seismic records contain information about the effect of the source as well as the effect of wave propagation through the rock mass. The effect of wave propagation is usually not well known as only simplified models of geological structures are available. Therefore, the information about the source retrieved by inverting seismograms may include errors due to incomplete knowledge of the rock mass along the propagation path, which in turn cause a distortion in the calculated moment tensor (MT). The distortion of the MT on a local scale was observed by inverting records of a simulated rockburst conducted at the Kopanang gold mine in South Africa. A dominant isotropic component of the explosive characteristics was found from the inversion. The deviatoric components retrieved from the blast are spurious. A test of their stability indicated that they are not significant, assuming an uncertainty above 5% for velocities and 10% for attenuation within the homogeneous model available for the mine. Thus, the retrieval of the MT from records of local networks in mines using a homogeneous model of the rock mass seems to be feasible. However, the homogeneous model of the rock mass can only be applied to close stations, within a few kilometers of the source. The seismic records from distant stations were too complex to be modelled by a homogeneous rock mass. Records of six mine-induced seismic events recorded at the Kopanang gold mine were also inverted. A vertical linear dipole along the pressure (P) axis was found for three of the events, suggesting a pillar burst. The mechanism of two events contains an isotropic implosion together with a nearly vertical dip-slip, and seems to indicate a combination of a cavity collapse with a down dip-slip along a nearly vertical fault. One event corresponds to a dipole along the tensional (T) axis. However, it is vertical, thus its association with tensile faulting of the hangingwall is uncertain.

Key words: Mine-induced seismic events, mechanism, isotropic and deviatoric components, confidence due to velocity and attenuation perturbations.

Introduction

The determination of the mechanism of the seismic source and retrieval of the parameters of the earth's crust and mantle have been considered largely as independent topics. During the retrieval of the source mechanism, an averaged model of the geological structure between the source and receiver is usually accepted. Due to the coupling of source and propagation effects in seismic records, this is

[1] Geophysical Institute, Academy of Sciences, Bocní II/1401 14131 Praha 4, Czech Republic.
[2] CSIR Mining Technology, P.O. Box 91230, Auckland Park 2006, Johannesburg, South Africa.

possible only for long-period seismic waves, which do not "see" the details of the structure. This approach is acceptable in the inversion of teleseismic waves originated from strong earthquakes with magnitudes greater than six, as used in the Harvard CMT catalogue (DZIEWONSKI *et al.*, 2001) as well as in the routine procedure of the United States Geological Survey (SIPKIN *et al.*, 2002). Similarly, it is realistic to retrieve moment tensors of moderate earthquakes from long-period waves recorded at regional distances. The catalogue of the Swiss Seismological Survey lists the CMT solutions of the events from the Mediterranean region with moment magnitudes greater than three (BRAUNMILLER *et al.*, 2002), the catalogue based primarily on MEDNET data contains hundreds of events as well (PONDRELLI *et al.*, 2002). The MTs of regional events in the western Mediterranean are summarized by STICH *et al.* (2003). The moderate regional events around Japan are documented in the NIED catalogue by KUBO *et al.* (2002). Several case studies were performed to invert short-period records originated by weak earthquakes (SCHURR and NABELEK, 1999; FERDINAND and ARVIDSSON, 2002). However, the resolved mechanism does not seem to be completely stable when different pass-bands are considered in the range of periods recorded by SP instruments. Simulation of adequately complex records by using available simple earth models is very difficult in the high-frequency band. The less affected parameters of the seismograms such as amplitudes of first onsets or polarities (OGASAWARA *et al.*, 2002) should then be used. The amplitude of the low-frequency plateau in the spectral domain may be evaluated from integrals of displacement and velocity records (TRIFU *et al.*, 2000; TRIFU and SHUMILA, 2002a, b). Contrary to complex SP regional records, the seismograms at stations close to the hypocenter are often fairly simple. Most of mining-induced seismic events at close distances fall within this category. They are considerably weaker than tectonic earthquakes, and the seismic waves can only be recorded at short distances. Along a short path their velocity is less variable than on the regional scale and is frequently assumed to be constant. This is an implicit assumption made in some studies of seismicity in mines (TRIFU, 2002). The assumption is only valid to wavelengths longer than the characteristic length of small-scale tectonic discontinuities. Blocks formed by fractures act as scatterers for short-period waves. These structures are generally difficult to map and, therefore, there is no chance of describing the rock mass deterministically on this scale. The characteristic length of small-scale tectonic discontinuities is thus the threshold for the description of the rock mass. Above this length, the concept of a simple homogeneous medium is acceptable as a good approximation, and, below this length the medium should be treated as a stochastic phenomenon.

The homogeneous medium accepted for wavelengths above the characteristic length is an average of the properties of small-scale units. These parameters should be considered with some uncertainties around the average values. For instance, in Canadian mines the uncertainty in velocity does not exceed 5–7% (TRIFU, 2004). A realistic estimate of velocity uncertainties could be used in cases when such

measurements are not available. In this study, we assumed that the error in the P- and S-waves velocities ranged from 5% to 10%. A more adequate model for both close and distant stations, which display different prevailing periods, can be obtained by including the attenuation in the rock mass. Uncertainties in the Q parameter are estimated in a similar way as uncertainties in the velocities. A higher percentage was used for the attenuation as it is generally less well known than the velocity.

In the first approximation, we assume a Gaussian distribution for the parameters of the homogeneous rock mass model with the standard deviation equal to a pre-set percentage. For several trials, we construct Green's functions for the model parameters randomly chosen from the above distributions. We invert the records by using this Green's function, and then map the uncertainty of the source mechanism, the source time function and the scalar moment of the obtained solutions.

In particular, we are interested in assessing the accuracy of the shear vs. non-shear components in the mechanism. It has been pointed out in the literature that non-DC components of earthquake sources may be artifacts of: inaccurate modelling of the crust or imperfect location (KUGE and LAY, 1994); oversimplifying the inhomogeneity of the crust (KRAVANJA *et al*., 1999); neglecting anisotropy (ŠÍLENÝ and VAVRYCUK, 2000, 2002) or neglecting reflected phases at discontinuities next to the source (ŠÍLENÝ *et al*., 2001). The question of validity of the retrieved non-DC components may be even more important at foci of mine-induced seismic events. In the complex stress environment around mine openings a more complex fracture process is expected compared to the simple shear slip along a pre-existing fault plane (HASEGAWA *et al*., 1989). To test the resolution, it is useful to invert seismograms generated by a controlled source, with a known mechanism. This can be achieved by a blast modelled as an isotropic explosive source. At regional distances, this inversion experiment has been performed with seismic records of a calibration blast, detonated on November 11, 1999 in the Dead Sea (ŠÍLENÝ and HOFSTETTER, 2002). The aim of the calibration blast was to constrain the 1-D velocity structure in this region for location purposes. It was found that complexities of the blasting in water masked the isotropic source process, and a spurious nearly DC mechanism appeared. The present simulated rockburst—a blasting experiment carried out in a deep-level gold mine—was performed within a rock mass. Thus, this experiment was much more suitable for testing the resolvability of the individual source components. Several mine-induced seismic events accompanying the simulated rockburst were also processed using the same method. Their non-shear mechanisms in terms of the rockburst models reported by HASEGAWA *et al*. (1989) are discussed.

Method

Waveforms in the time domain were inverted by a method using indirect parameterization (INPAR) of the point source (ŠÍLENÝ *et al*., 1992; ŠÍLENÝ, 1998).

First, waveforms are inverted into Moment Tensor Rate Functions (MTRFs) by the optimum filter design method (SIPKIN, 1982), which are reduced subsequently into the joint Source Time Function (STF) and Moment Tensor (MT). The solution of any inverse problem includes some uncertainty. The source of errors may be due to noise in the records, or may represent an error in the forward modelling, such as uncertainty in the description of the rock mass properties, or error in the seismic location. Uncertainty in forward modelling in a mine environment due especially to the presence of cavities underground can be partly reduced by group processing of the data (DAHM *et al.*, 1999; ANDERSEN and SPOTTISWOODE, 2001; LINZER, 2005)

A high signal-to-noise ratio was observed in the seismograms recorded by the Klerksdorp seismic network. The hypocenter of the simulated rockburst is known, and the location error of mine-induced seismic events is comparatively small. On the other hand, uncertainties in the rock mass properties may be expected. The parameters of the homogeneous model represent average values across the span of small-scale heterogeneities. They display a scatter around these values and can be considered to be random variables. The velocities V_P and V_S and attenuation parameters Q_P and Q_S with the standard deviation equal to an *a priori* specified percentage of the average value were considered to have a Gaussian distribution.

Multiple inversion by using a perturbed rock mass model allows the estimation of STF and MT confidence zones. The reliability of the MT is described by four confidence zones. Three of them are related to the T, N and P axes and contain information about the reliability of the orientation of the Fault Plane Solution (FPS). The fourth zone indicates how reliably individual elementary mechanisms in the complete MT, namely the Isotropic Source (ISO) describing an explosion or implosion, the Double-Couple (DC) corresponding to a shear slip along the fault plane, and the Compensated Linear Vector Dipole (CLVD) are determined. The MT as described by RIEDESEL and JORDAN (1989) was used (RJ). The content of each of the elementary mechanisms in the retrieved MT is visualized by the distance of descriptive points for the MT and the ISO, DC and CLVD mechanisms on the projection of the focal sphere. For instance, if the MT confidence zone modelled by the cloud around the MT contains the DC descriptive point, then the retrieved moment tensor can be regarded as a pure DC source (Fig. 1).

Data

A simulated rockburst was conducted underground at the Kopanang gold mine in the Klerksdorp region, South Africa. The experiment was carried out in September 1998, in order to investigate the rockburst damage mechanism and site

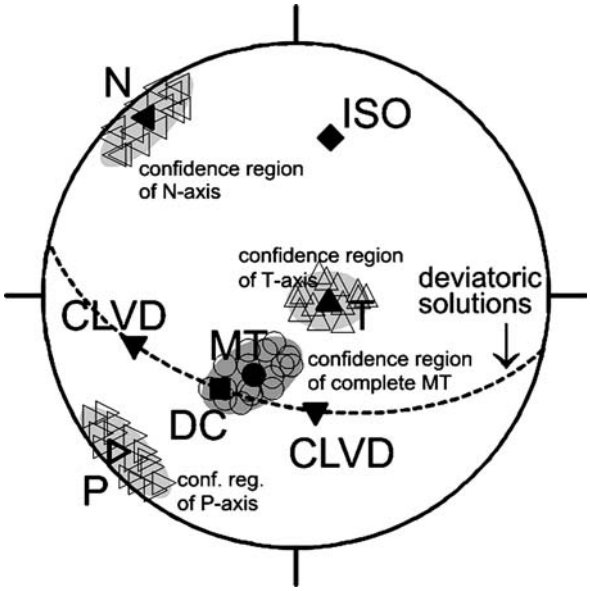

Figure 1
Display of decomposition of seismic moment tensor and corresponding uncertainty by RIEDESEL and JORDAN (1989). Complete moment tensor and the elementary mechanisms related to decomposition are marked by: MT - circle, ISO - diamond, DC - square and CLVD - triangle down. The proximity of the MT projection to ISO, DC and CLVD projections expresses the amount of the isotropic component, double-couple and compensated linear vector dipole in the complete moment tensor. The dashed line displays the locus of deviatoric moment tensors. The principal axes are marked by: T axis – triangle up, N axis – triangle left and P axis - triangle right. By stacking moment tensors obtained from inversions using the perturbed rock mass model, the uncertainty in the solution expressed by confidence regions can be displayed. Uncertainty in the orientation of the deviatoric part of the moment tensor is expressed by confidence regions of T, N and P axes. Uncertainty in the moment tensor decomposition is shown by the confidence region of the vector MT.

response to strong ground motion. The rockburst was simulated by a large explosion detonated in solid rock close to a sidewall of an underground tunnel (Fig. 2). The research undertaken by HAGAN *et al*. (2001) comprised the following areas: forward and back analysis of the simulated rockburst using numerical modelling (HILDYARD and MILEV, 2001); the installation of a micro-seismic array near the source and seismic monitoring in the far-field by the Klerksdorp regional network (MILEV *et al*., 2001); high-speed video filming to derive the ejection velocities (RORKE and MILEV, 1999); a study of rock mass conditions (fractures, joints, rock strength, etc.) before and after the blast to estimate the extent and type of damage (REDDY and SPOTTISWOODE, 2001; GRODNER, 2001), and evaluation of the support performance under dynamic loading (HAILE and LE BRON, 2001).

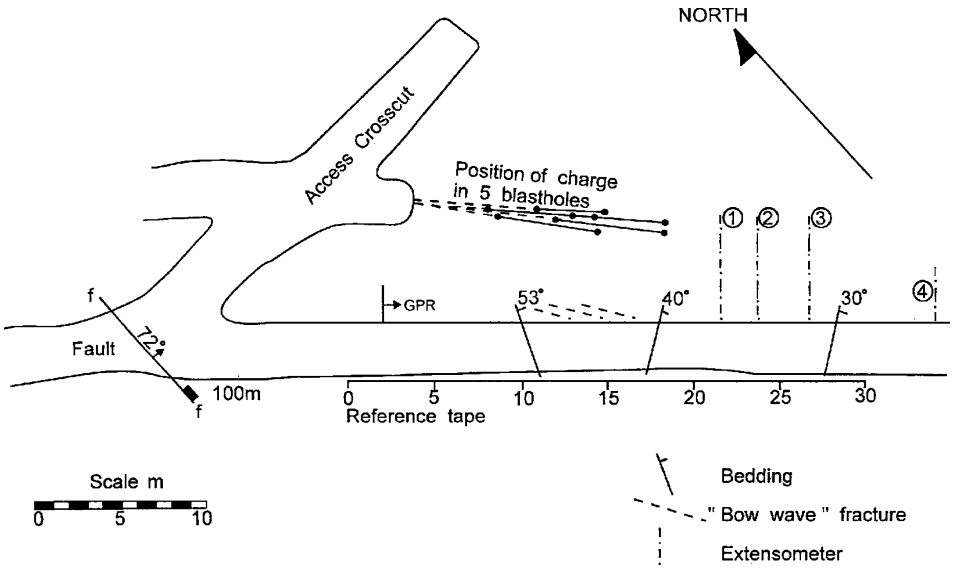

Figure 2
Plan view of the underground tunnel used in the simulated rockburst experiment (HAGAN *et al.*, 2001). Position of the blasting holes and the main discontinuity of the tunnel wall are shown in the plan.

The simulated rockburst and seismic events investigated in this study were observed by the Klerksdorp regional seismic network. Most events were recorded by 16 seismic stations located underground, with hypocentral distances ranging from 850 m to about 9.5 km with a rather sparse coverage of the focal sphere (Fig. 3). The transducers used in the seismic stations were 4.5 Hz geophones grouted in the solid rock. This type of geophone has a flat frequency amplification curve above 4.5 Hz. Since the frequency range of the records falls within the flat response of the geophones, further correction of the signals was not necessary. A low-pass Butterworth filter at 20 Hz was then applied to simplify the signals (Fig. 4). Windows in duration of 0.1 sec containing P and S waves were selected starting at the corresponding arrival times.

The data currently available for the rock mass are seismic wave velocities $V_P = 5800$ m/s and $V_S = 3500$ m/s, and density $\rho = 2700$ kg/m^3. By comparing the frequency content of the signals recorded close and far from the hypocenter, it was found that the medium absorbs the high frequencies far from the hypocenter (Fig. 4). Thus, the elastic Green's function could not fit the close and distant station records simultaneously, because it predicts the same frequency regardless of the distance. In several trials we attempted to allocate values of Q for P and S waves, which yielded the best fit of synthetic to observed data at both close and distant stations. Values of $Q_P = 100$ and $Q_S = 166$ providing equal attenuation of P and S waves were applied. A reasonable fit of synthetic and observed data

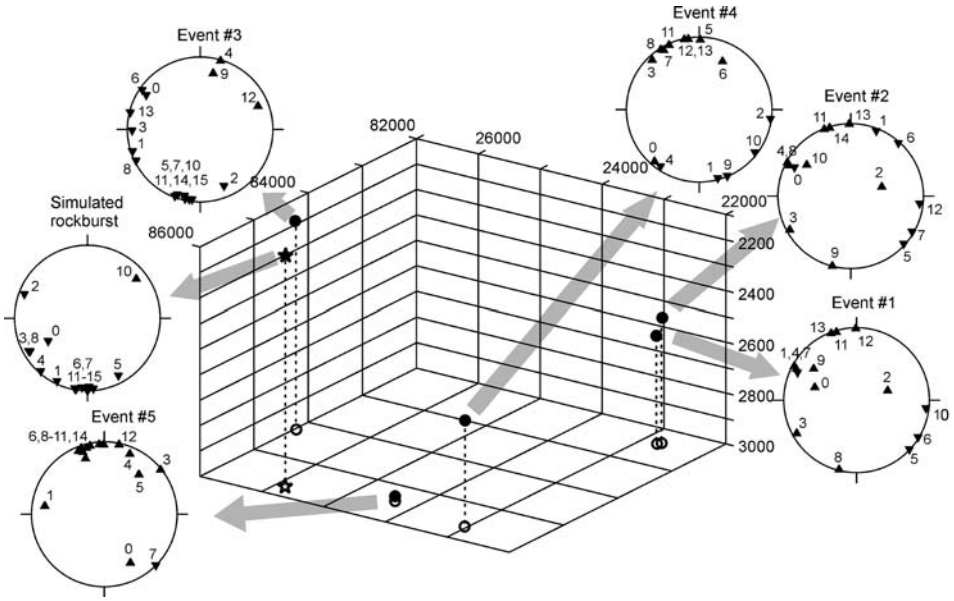

Figure 3
Map of hypocenters of the simulated rockburst (asterisk) and five seismic events (circles) recorded in the Kopanang gold mine. In the insets for each event the focal sphere coverage is displayed by stations of the Klerksdorp regional seismic network. Equal area projection of the lower focal hemisphere was used.

was found for stations at distances up to 4.5 km (Fig. 5). The stations farther from the hypocenter could not be modelled satisfactorily. This was attributed to the fact that the simple homogeneous rock mass model is not adequate for longer distances.

Results

Simulated Rockburst

The duration and complexity of the waveforms increase with hypocenter distance, which suggests that the homogeneous model of the rock mass is not adequate at distances far from the hypocenter. In inverting the complete data, we found that records at stations farther than 4.5 km did not match well. Excluding those records from the data set did not change the result, as the least-squares inversion preferably matches large amplitudes which appear at stations close to the hypocenter. The other source of discrepancy is a change of the frequency content with distance: The waveforms become more long-period, and therefore cannot be successfully modelled by the attenuation except for the stations within 4.5 km. The results presented below

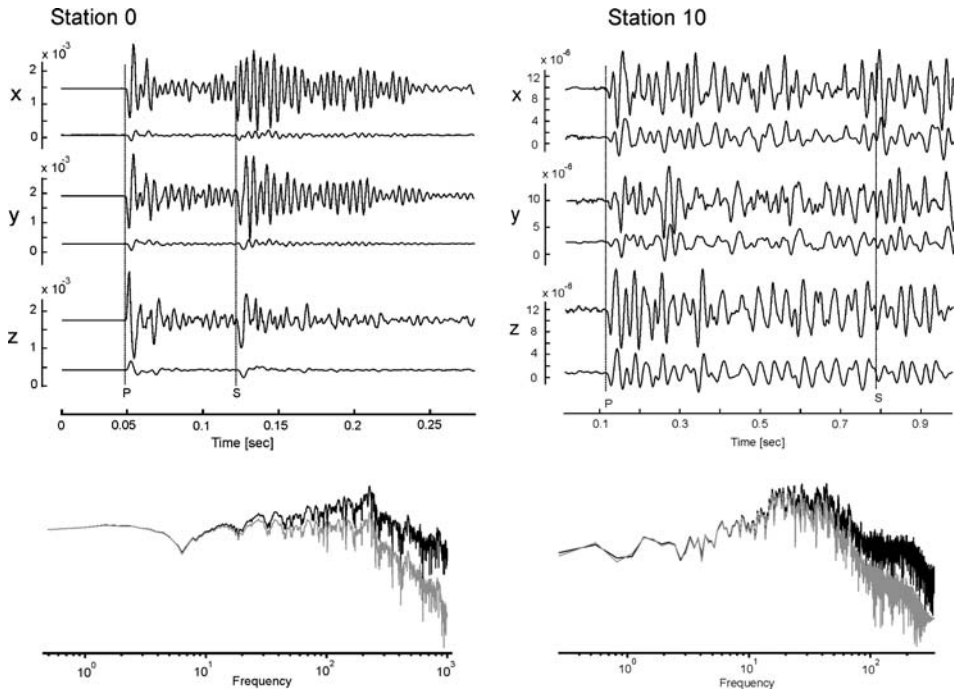

Figure 4
Seismograms recorded at Station 0 (distance 0.85 km to the source) and Station 10 (distance 6.14 km to the source). The upper trace is the original seismogram, the lower trace is filtered by a low-pass Butterworth filter at 20 Hz; the dotted line indicates the arrival time of P and S waves. The bottom plots are spectra of the Z component of the original seismogram (black line) and filtered seismogram (grey line).

correspond effectively to the inversion of stations within that distance, i.e., Stations 0 to 5.

The values of the parameters of the rock mass model available are only estimates of the real values. This introduces an uncertainty in the retrieved source which is described by the confidence zones of the mechanism and the source time function. Each individual solution is obtained by inverting the data using perturbed Green's function. For each perturbation, values of the rock mass model parameters are chosen randomly from the Gaussian distribution with the standard deviation set to a fixed percentage of the parameter value. We tested 5% and 10% uncertainty in velocities and uncertainties of 5% to 50% in Q. The simulated rockburst in the Kopanang mine was used to calibrate the uncertainty of the model parameters. A blast modelled as a point source in a homogeneous medium should have a spherical radiation for the P wave and will not radiate S wave. However, in case these conditions are not valid, the explosion is not a pure isotropic source and contains a deviatoric part as well. The simulated rockburst

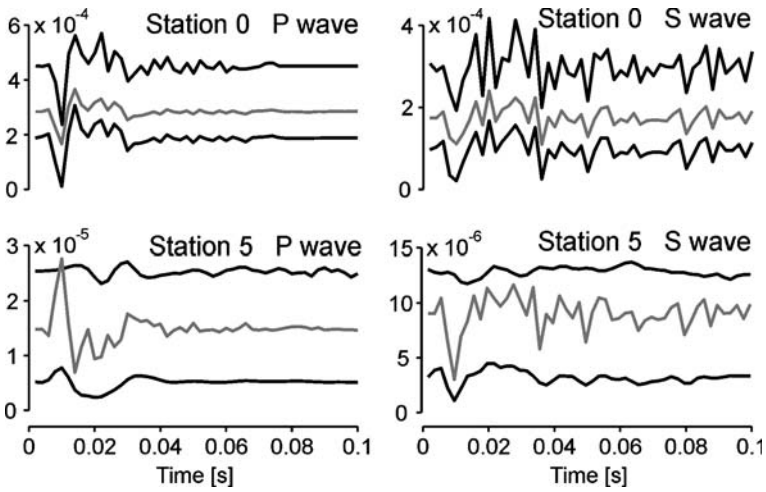

Figure 5
Effect of attenuation attributed *ad hoc* to the homogeneous model of the rock mass: Horizontal component at a close station (Station 0 at a distance of 853 m) and at a distant station (Station 5 at a distance of 4473 m). Observed vs. synthetic seismograms at Station 0 (top) and Station 5 (bottom). The P wave is on the left and S wave is on the right. The upper trace indicates the observed data; the middle trace (grey line) indicates the synthetic data without attenuation; and the lower trace indicates the synthetic data with attenuation $Q_P = 100$ and $Q_S = 166$.

was performed by detonating the explosives in several parallel drill-holes, constitutes a finite-size linear source rather than a point source. In addition, it was blasted in the wall of the underground tunnel (Fig. 2), where interaction with the free surface introduced converted waves in the wave field. For that reason, we expected the existence of an isotropic (explosive) component in the mechanism of the simulated rockburst. The amount of uncertainty of the medium was estimated by excluding a purely deviatoric source. To do this, we searched for the amount of perturbation of the parameters of the medium, which does not allow a purely deviatoric source in terms of the confidence region. This must remain well separated from the circle of deviatoric solutions. It is shown in Figure 6 that perturbations exceeding 5% in velocities and 10% in Q generate confidence regions which cross or touch the deviatoric circle. At these levels a pure deviatoric solution (a solution without isotropic component) is allowed. This indicates that perturbations of 5% in V_P and V_S and 10% in Q_P and Q_S are appropriate values for the Gaussian distributions of velocities and Q (Fig. 7). The unperturbed model yields a large prevalence of isotropic mechanism (58%), which completely removes the compressions from the focal sphere (Fig. 8a). The ISO component is complemented by 19% of DC and 23% of the CLVD along the T axis. The orientation of the deviatoric part is fairly stable, which can be seen from the tightly clustered nodal lines for the perturbed models (Fig. 8b). This indicates that

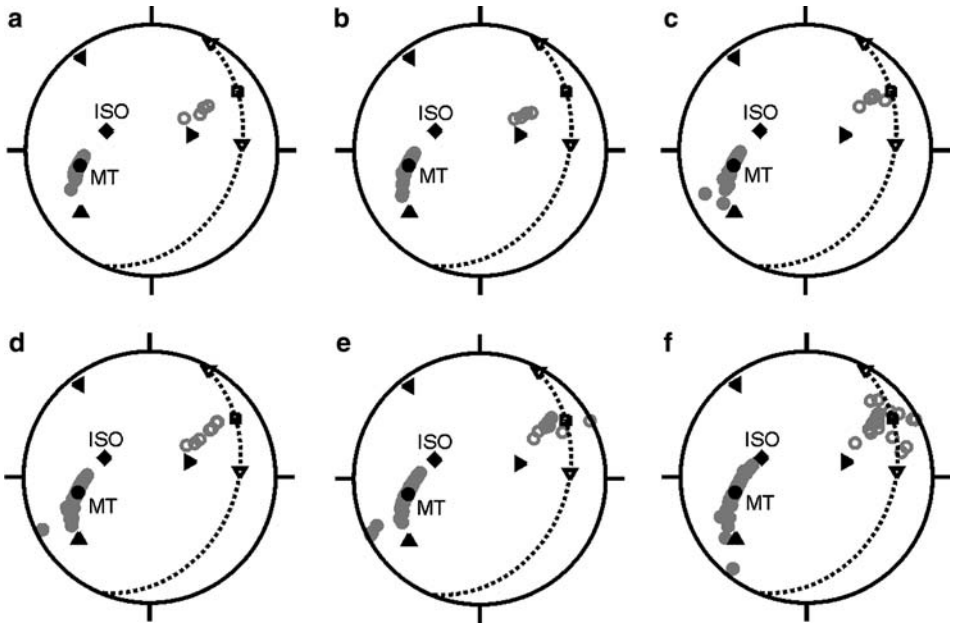

Figure 6
(a–f). Simulated rockburst, confidence regions for various uncertainties in modelling the rock mass by a homogeneous model. Velocities and attenuation are considered as random variables with a Gaussian distribution around average values of $V_P = 5800$ m/s and $V_S = 3500$ m/s, $Q_P = 100$ and $Q_S = 166$ with standard deviation equal to an *a priori* specified percentage of the average. a) 5% for both V and Q; b) 5% for V and 10% for Q; c) 10% for both V and Q; d) 5% for V and 20% for Q; e) 5% for V and 30% for Q; f) 5% for V and 50% for Q. For details of the display see the caption of Figure 5.

the deviatoric part of the mechanism is not an artefact of the mismodelling of the rock mass, and most probably is associated with the mechanism of the simulated rockburst. In the STF a significant dominant peak is determined which is present in all perturbations, while the remaining peaks are insignificant as they are non-zero for some of the perturbations only (Fig. 8c). The changes of MT and STF during the perturbing of the medium result in fluctuation of the scalar moment M_0. However, its distribution is reasonably smooth and there is a single peak which allows reliable determination of M_0 around values of 4×10^8 Nm (Fig. 8d).

Mine-induced Seismic Events

Five mining-induced seismic events located in the same geotechnical area as the simulated rockburst experiment were analyzed using the same methodology. Results are summarized in Figures 9 to 13. The following diagrams are shown for each event: (a) the focal sphere coverage; (b) fault plane solution showing the orientation of the

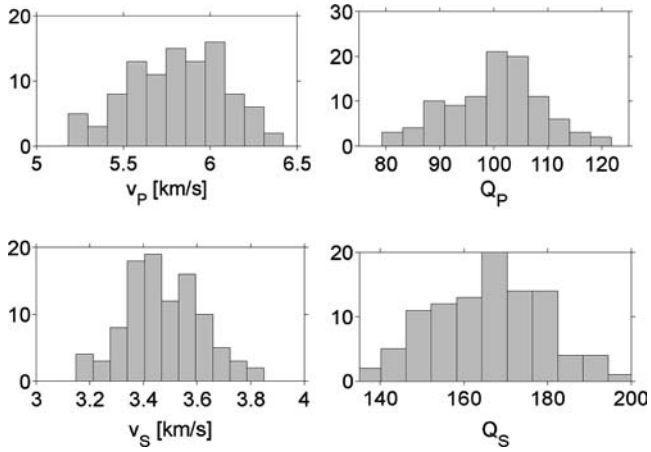

Figure 7
Histograms of distributions of V_P, V_S, Q_P and Q_S modelled from 100 samples taken from the Gaussian distribution with standard deviation equal to 5% of the mean value for velocities and to 10% of the mean value of attenuation.

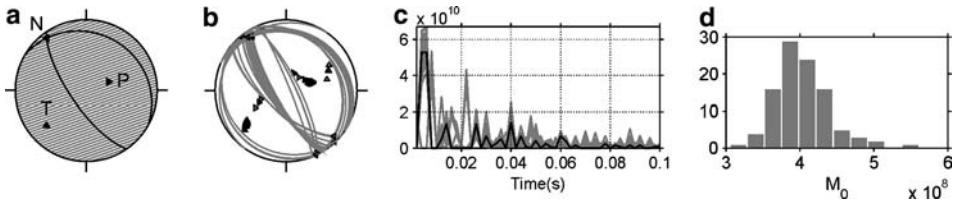

Figure 8
Simulated rockburst: a) Conventional plot of mechanism obtained from the unperturbed model: fault-plane solution (nodal lines of the DC part), and the zone of compressions (grey area) corresponding to the complete moment tensor; b) scatter of fault-plane solutions due to variation of the model (5% in velocities and 10% in Q); c) scatter of source time function; d) histogram of the values of scalar moment corresponding to the individual solutions with the perturbed model.

DC part of the mechanism together with zone of compression influenced by the complete MT, as a result it does not follow the nodal lines of the FPS; (c) the set of nodal lines corresponding to solutions with perturbed rock mass model, which illustrate the stability of the FPS, as well as a set of MT solutions in the R-J display which shows the stability of the ISO, DC and CLVD components in the retrieved MT; (d) histogram of the values of scalar moment; and (e) set of source time functions.

The percentage of the uncertainty of the medium model was calibrated by the simulated rockburst. The stability of the solutions is fairly high both as concerns the FPS orientation and the contents of the ISO, DC and CLVD components. The

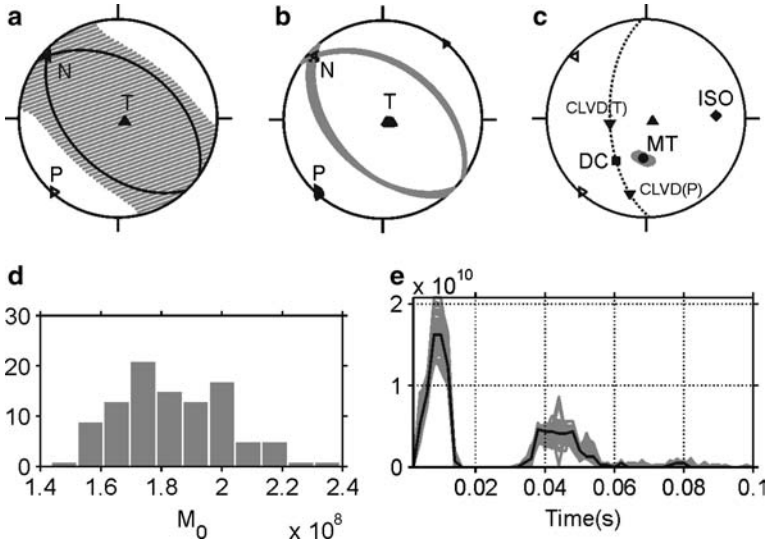

Figure 9
Event 1: a) Mechanism derived from the unperturbed model; b) scatter of fault-plane solutions due to variation of the model (5% in velocities and 10% in Q); c) RJ-plot of moment tensors corresponding to the perturbation of the model; d) histogram of M_0 values corresponding to the individual solutions with the perturbed model; e) scatter of the source time function due to the model perturbation.

bundles of nodal lines are very tight, allowing a rotation only within several degrees. The confidence zone of the moment tensor estimated by the cloud of points around the MT point in the R-J display is small, hence, the percentage of the individual source components is almost fixed (Table 1). All solutions were determined as non-DC, even non-deviatoric. In the R-J plots of each event the MT confidence zone stays distinctly out of the locus of deviatoric solutions.

Event 1 is prevalently a shear slip of 67% with nearly 45° dip-slip orientation (Fig. 9). Its non-DC components may be less significant, because the MT confidence region approaches the DC elementary mechanism in the R-J display closest from all the events investigated. The STF is nearly a single peak because the other lobe (between 0.03 s and 0.05 s) is less resolved owing to the scatter of the individual solutions (Fig. 9e). However, the M_0 value is rather uncertain, as its distribution is rather wide and is not smooth, (Fig. 9d).

Events 2, 3 and 4 are similar in the MT decomposition: (i) dominant CLVD along P axis oriented vertically; (ii) large isotropic implosion; and (iii) very small DC component. The M_0 distributions are fairly smooth, yielding reliable estimates of the scalar moment. However, the STF is simple only for Event 3. Events 2 and 4 show more additional peaks which cannot be simply discarded. Their amplitudes are large and the scatter of their individual solutions is small (Figs. 10e and 12e). There is no obvious reason for this complexity. Since all the events analyzed in this study have

Table 1

Decomposition of moment tensors of events analyzed

Event Number	Location			Moment tensor decomposition		
	South	West	Depth	ISO [%]	DC [%]	CLVD [%]
Simulated Rockburst	85647	25926	2114	58 (explosive)	19	23 (along T-axis)
Event 1	82402	22772	2574	25 (explosive)	67	8 (along P-axis)
Event 2	82371	22716	2501	39 (implosive)	11	50 (along P-axis)
Event 3	84262	26972	2186	33 (implosive)	10	57 (along P-axis)
Event 4	85605	23059	2578	26 (implosive)	8	66 (along P-axis)
Event 5	85455	24322	2980	36 (implosive)	53	11 (along T-axis)

small magnitudes, multiple source rupture is not likely to be the reason for the complicated solution. The complexity is probably an effect of inaccurate forward modelling where a simple rock mass structure was used.

Event 5 contains a combination of DC, oriented as a nearly vertical dip-slip, with a large isotropic implosion (Figs. 13a and 13c). Both M_0 and STF patterns are simple and have a single peak which is well resolved in the latter case (Fig. 13e).

Discussion

The source mechanisms, source time function and scalar moments of five seismic events located in the Kopanang gold mine were determined. The seismic events

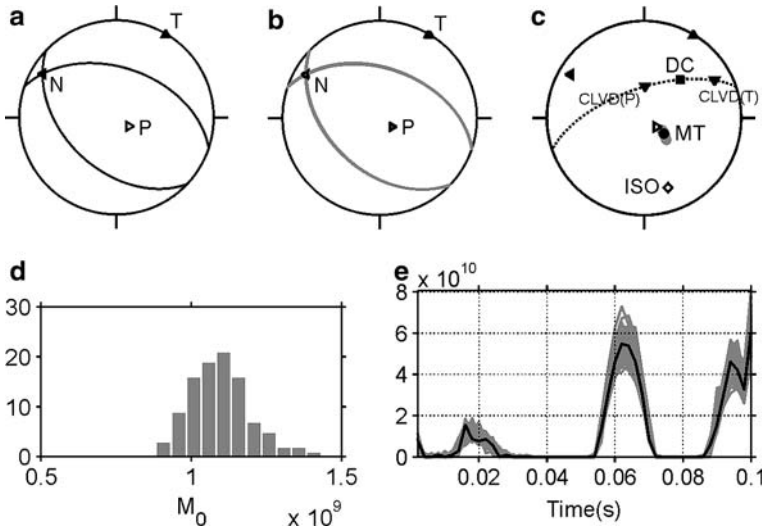

Figure 10
Event 2. For details see caption of Figure 9.

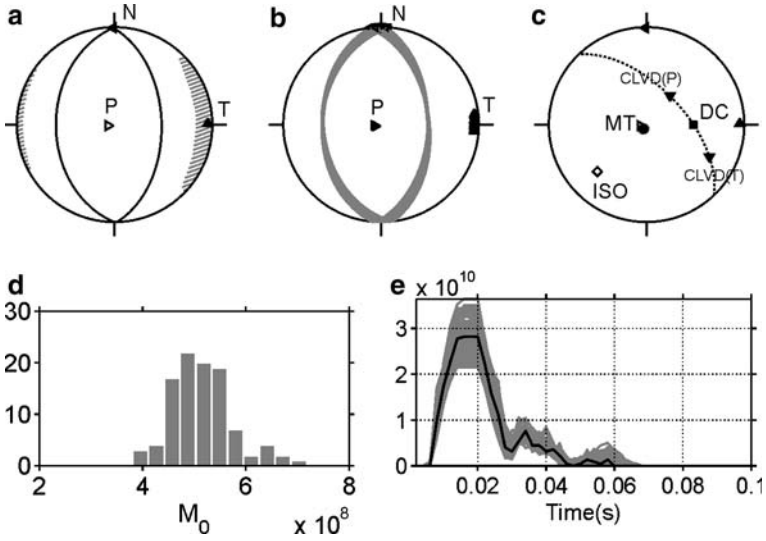

Figure 11
Event 3. For details see caption of Figure 9.

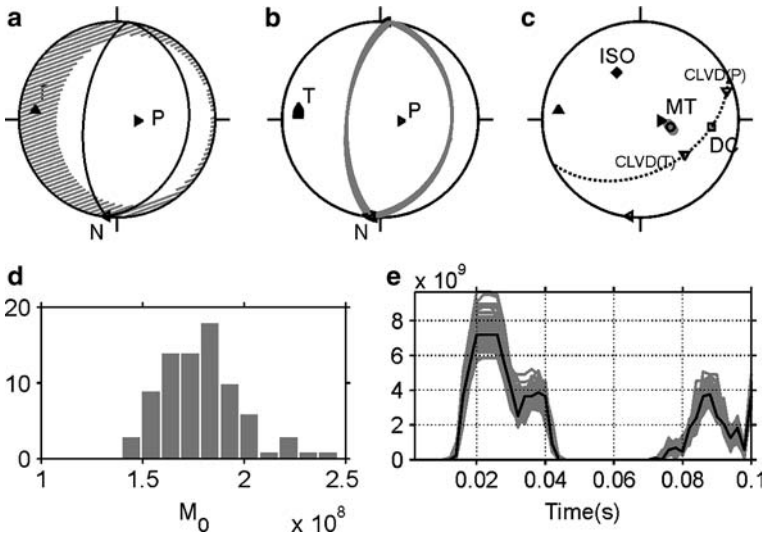

Figure 12
Event 4. For details see caption of Figure 9.

recorded underground were processed assuming a homogeneous rock mass model. However variable velocities and attenuation were considered.

The values of V_P, V_S, Q_P and Q_S were allowed to vary within the Gaussian distribution around average values. As the scatter of the rock mass parameters is

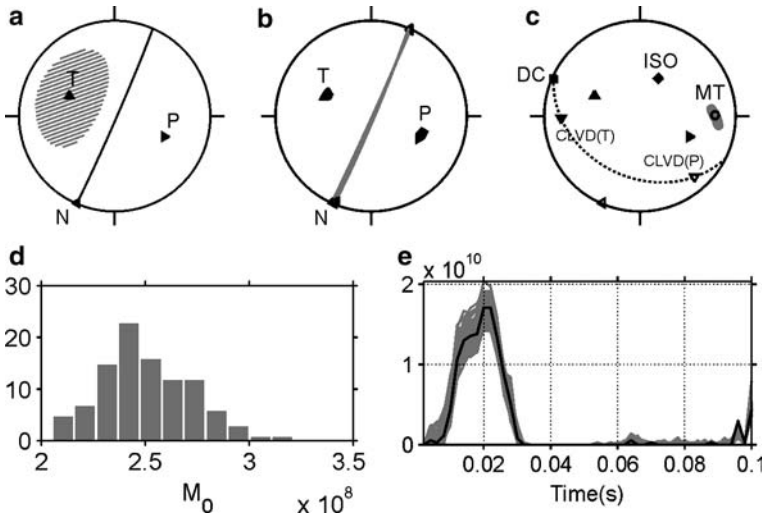

Figure 13
Event 5. For details see caption of Figure 9.

usually not well known, we applied a fixed percentage of the average value for the standard deviation of distribution. To determine the percentage, we used the experiment with inversion of the simulated rockburst. The requirement of its non-deviatoric mechanism yielded a percentage of 5% for velocity and 10% for attenuation mismodelling. Using these values, we constructed estimates of confidence regions for the principal axes and the decomposition of the moment tensors of five seismic events. We found that the orientation and the percentage of the individual MT components were determined with a high certainty. The orientation of the mechanism remains within several degrees, and the DC, CLVD and ISO components are determined within an accuracy of several percent. This accuracy is too high to be realistic and is probably due to neglecting effects of inhomogeneity and anisotropy in the rock mass modelling. These effects can lead to an additional error imposed on the source parameters.

The mechanism of these seismic events was compared to the systems of dipoles obtained with models suggested by HASEGAWA *et al.* (1989) (Fig. 14). An explosive isotropic component was only obtained in the mechanism of Event 1. It forms a part of the equivalent body force of a tensile crack or a tensional fault, which is one of the Hasegawa *et al.* models. They attribute it to the failure of the hangingwall overlying a mine cavity, which results in horizontal tension. On the contrary, our mechanism composed of an explosion and a DC component is oriented subvertically. The mechanisms of Events 2, 3 and 4 are similar. They consist of the combination of a large CLVD component along the P axis oriented

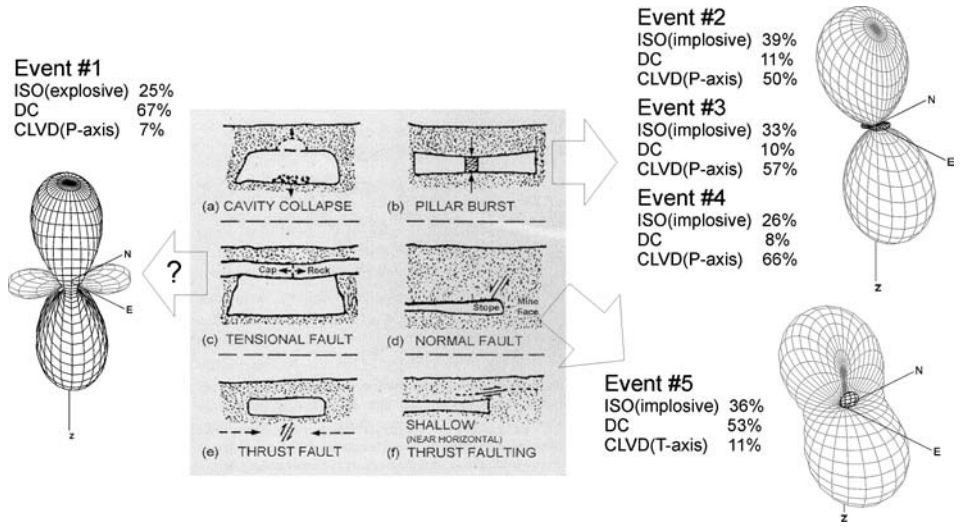

Figure 14
Mechanisms of Events 1 to 5 displayed by using 3-D wire-frame plots of their P-wave radiation patterns (black lines are positive amplitudes and grey lines are negative amplitudes), and their correlation with rockburst models by HASEGAWA *et al.* (1989). For each event the decomposition of the moment tensor into ISO, DC and CLVD are presented.

subvertically and an implosive isotropic part, while the DC is very small. This mechanism approached closely a vertical pressure dipole, which has 66.6% of the CLVD along the P axis, 33.3% of isotropic implosion and no DC. A vertical pressure dipole can be associated with a pillar burst (MALOVICHKO, 2005a,b). Event 5 is a combination of an isotropic implosion and a DC, with only small portion of CLVD. This corresponds to the Hasegawa *et al.* model, which combines a normal shear slip along an inclined fault close to a cavity. The fault plane solution found for this event consists of a normal fault inclined very steeply, dipping at an angle of 88^0.

Conclusions

1. By using the simulated rockburst at a deep-level gold mine as a controlled explosion event, we calibrated the parameters of homogeneous rock mass. Uncertainty of 5% in seismic velocities and 10% in Q yield the non-deviatoric mechanism consistent with the blast.
2. Among moment tensors of five mining tremors from the mine, three are mostly single couples along nearly vertical pressure axis, which may correspond to pillar bursts. One combines implosion with a DC, which may reflect cavity collapse due

to a shear slip nearby. One is mostly single couple along a vertical tensional axis, suggesting a horizontal tensile crack.

3. Errors of the retrieved mechanism based on perturbation of the homogeneous rock mass model are very small and may be underestimated by neglecting the inhomogeneity and anisotropy of the rock mass.

Acknowledgements

The Czech Academy of Sciences Grant Agency supported the project under Grant No. IAA300120502. The blasting experiment was part of the research program supported by SIMRAC now MSHC (Mine Safety and Health Council) of South Africa, under Project GAP 530. The authors gratefully acknowledge Dr Lindsay Linzer of CSIR Mining Technology reviewing the manuscript. Comments of the reviewers Prof. Eliza Richardson and Dr. Cezar I. Trifu improved the paper greatly.

References

Andersen, L.M., and Spottiswoode, S.M., *A hybrid relative moment tensor methodology*. In (G. van Aswegen, R.J. Durrheim, and W.D. Ortlepp, eds.) *Rockbursts and Seismicity in Mines* RaSim5 (The South African Institute of Mining and Metallurgy Balkema 2001), pp. 81–90.

Braunmiller, J., Kradolfer, U., Baer, M., and Giardini, D. (2002), *Regional moment tensor determination in the European–Mediterranean area—Initial results,* Tectonophysics *356*, 5–22.

Dahm, T., Manthei, G., and Eisenblätter, J. (1999), *Automated moment tensor inversion to estimate source mechanisms of hydraulically induced micro-seismicity in salt rock*, Tectonophysics *306*, 1–18.

Dziewonski, A.M., Ekström, G., and Maternovskaya, N.N. (2001), *Centroid-moment tensor solutions for July – September 2000*, Phys. Earth Planet. Int. *124*, 9–23.

Ferdinand, R.W. and Arvidsson, R. (2002), *The determination of source mechanisms of small earthquakes and revised models of local crustal structure by moment tensor inversion*, Geophys. J. Int. *151*, 221–234.

Grodner, M. (2001), *Using Ground Penetrating Radar to quantify changes in the fracture pattern associated with a simulated rockburst experiment*, J. of South Afr. Inst. of Mining and Metallurgy *101*, 261–266.

Hagan, T.O., Milev, A.M., Spottiswoode, S.M., Hildyard, M.W., Grodner, M., Rorke, A.J., Finnie, G.J., Reddy, N., Haile, A.T., LeBron, K.B. and Grave, D.M. (2001), *Simulated rockburst experiment – An overview*, J. of South Afr. Inst. of Mining and Metallurgy *101*, 217–222.

Hasegawa, H.S., Wetmiller, R.J. and Gendzwill, D.J. (1989), *Induced seismicity in mines in Canada – An overview*, Pure Appl. Geophys. *129*, 423–453.

Haile, A.T. and Le Bron, K.B. (2001), *Simulated rockburst experiment – evaluation of rock bolt reinforcement performance*, J. of South Afr. Inst. of Mining and Metallurgy *101*, 247–252.

Hildyard, M.W. and Milev, A.M. (2001), *Simulated rockburst experiment development of a numerical model for seismic wave propagation from the blast, and forward analysis*, J. of South Afr. Inst. of Mining and Metallurgy *101*, 235–245.

Hildyard, M.W. and Milev, A.M. (2001), *Simulated rockburst experiment numerical back-analysis of seismic wave interaction with the tunnel*, J. of South Afr. Inst. of Mining and Metallurgy *101*, 223–234.

KRAVANJA, S., PANZA, G.F., and ŠÍLENÝ, J. (1999), *Robust retrieval of a seismic point-source time function*, Geophys. J. Int. *136*, 385–394.

KUBO, A., FUKUYAMA, E., KAWAI, H., and NONOMURA, K. (2002), *NIED seismic moment tensor catalogue for regional earthquakes around Japan: Quality test and application*, Tectonophysics *356*, 23–48.

KUGE, K. and LAY, T. (1994), *Data-dependent non-double-couple components of shallow earthquake source mechanisms: Effects of waveform inversion instability*, Geophys. Res. Lett *21*, 9–12.

LINZER, L.M. (2005), *A relative moment tensor inversion technique applied to seismicity induced by mining,* J. Rock Mechanics and Rock Engineering *38*, 81–104.

MALOVICHKO, D.A. (2005a), *Description of Mine-Related Seismic Events*, Phys. of the Solid Earth *41*, 853–859.

MALOVICHKO, D.A. (2005b), Mining Institute, Ural Branch, Russian Acad. Sci., 614007 Perm, Russia, personal communication.

MILEV, A.M., SPOTTISWOODE, S.M., RORKE, A. J., and FINNIE, G.J. (2001), *Seismic monitoring of a simulated rockburst on a wall of an underground tunnel*, J. of South Afr. Inst. of Mining and Metallurgy *101*, 253–260.

OGASAWARA, H., FUJIMORI, K., KOIZUMI, N., HIRANO, N., FUJIWARA, S., OTSUKA, S., NAKAO, S., NISHIGAMI, K., TANIGUCHI, K., IIO, Y., NISHIDA, R., OIKE, K. and TANAKA, Y. (2002), *Microseismicity induced by heavy rainfall around flooded vertical ore veins*, Pure Appl. Geophys. *159*, 91–110.

PONDRELLI, S., MORELLI, A., EKSTRÖM, G., MAZZA, S., BOSCHI, E., and DZIEWONSKI, A. M. (2002), *European-Mediterranean regional centroid-moment tensors: 1997–2000*, Phys. Earth Planet. Int. *130*, 71–101.

RIEDESEL, M.A. and JORDAN, T.H. (1989), *Display and assessment of seismic moment tensors,* Bull. Seismol. Soc. Am. *79,* 85–100.

REDDY, N. and SPOTTISWOODE, S.M. (2001), *The influence of geology on a simulated rockburst experiment*, J. of South Afr. Inst. of Mining and Metallurgy *101*, 267–272.

RORKE, A.J. and MILEV, A.M. (1999), *Near Field Vibration Monitoring and Associated Rock Damage*, FRAGBLAST 1999, Johannesburg, South African Institute of Mining and Metallurgy.

SCHURR, B. and NABELEK, J. (1999), *New techniques for the analysis of earthquake sources from local array data with an application to the 1993 Scotts Mills, Oregon, aftershock sequence*, Geophys. J. Int. *137*, 585–600.

ŠÍLENÝ, J. (1998), *Earthquake source parameters and their confidence regions by a genetic algorithm with a "memory"*, Geophys. J. Int. *134*, 228–242.

ŠÍLENÝ, J. and HOFSTETTER, R. (2002), *Moment tensor of the 1999 Dead Sea calibration shot: Limitations in the isotropic source retrieval without a detailed earth model*, Tectonophysics *356*, 157–169.

ŠÍLENÝ, J., PCENCÍK, I. and YOUNG, R.P. (2001), *Point-source inversion neglecting nearby free surface: simulation of the Underground Research Laboratory, Canada,* Geophys. J. Int. *146*, 171–180.

ŠÍLENÝ, J., PANZA, G.F. and CAMPUS, P. (1992), *Waveform inversion for point source moment tensor retrieval with variable hypocentral depth and structural model*, Geophys. J. Int. *109*, 259–274.

ŠÍLENÝ, J. and VAVRYČUK, V. (2000), *Approximate retrieval of the point source in anisotropic media: numerical modelling by indirect parameterization of the source*. Geophys. J. Int. *143*, 700–708.

ŠÍLENÝ, J. and VAVRYČUK, V. (2002), *Can unbiased source be retrieved from anisotropic waveforms by using an isotropic model of the medium?* Tectonophysics *356*, 125–138.

SIPKIN, S.A. (1982), *Estimation of earthquake source parameters by the inversion of waveform data: Synthetic waveforms*, Phys. Earth Planet. Int. *30*, 242–259.

SIPKIN, S.A., BUFE, C.G., and ZIRBES, M.D. (2002), *Moment-tensor solutions estimated using optimal filter theory: Global seismicity, 2000*, Phys. Earth Planet. Int. *130*, 129–142.

STICH, D., AMMON, C.J., and MORALES, J. (2003), *Moment tensor solutions for small and moderate earthquakes in the Ibero-Maghreb region*, J. Geophys. Res. *108* (B3), Art. No. 2148.

TRIFU, C.I., ANGUS, D. and SHUMILA, V. (2000), *A fast evaluation of seismic moment tensor for induced seismicity*, Bull. Seismol. Soc. Am. *90*, 1521–1527.

TRIFU, C.I. and SHUMILA, V. (2002a), *Reliability of seismic moment tensor inversions for induced microseismicity at Kidd Mine, Ontario*, Pure Appl. Geophys. *159*, 145–164.

TRIFU, C.I. and SHUMILA, V. (2002b), *The use of uniaxial recordings in moment tensor inversion for induced seismic events*, Tectonophysics *356*, 171–180.

TRIFU, C.I. (ed.) (2002), *The mechanism of induced seismicity*, Pure Appl. Geophys. *159*, 1–3.
TRIFU, C.I. (2004), *Engineering seismology group Canada Inc*, 1 Hyperion Court, Kingston, Ontario, Canada K7K 7G3, personal communication.

(Received July 9, 2003, accepted February 7, 2006)